NON-CONVENTIONAL APPLICATION OF ROBUST MATCHED-FIELD LOCALIZATION: SMALL APERTURE ARRAY AND MID-FREQUENCY SIGNALS

Brian F. Harrison

Naval Undersea Warfare Center
Newport, RI 02841 USA
e-mail: harrison_bf@ieee.org

ABSTRACT

Conventional applications of matched-field processing (MFP) use large aperture vertical arrays and low frequency signals. It is well known that MFP's sensitivity to environmental mismatch is proportional to frequency. Thus, real-world application of MFP to mid-frequency signals, e.g., $800 - 3000$ Hz, is generally regarded a very difficult problem. Using small aperture vertical arrays can also compromise the performance of MFP. However, small aperture vertical arrays are more practical for real-world scenarios. In this paper, we propose the broadband L_∞-norm estimator for robust broadband matched-field localization of mid-frequency signals received on extremely small aperture vertical arrays. Results using a simulated Gulf of Mexico environment for broadband signals ($1000-3000$ Hz) received on a 3-meter vertical array demonstrate the significant performance gains in using the L_∞-norm estimator over the asymptotically-optimal maximum *a posteriori* estimator in the presence of finite environmental sampling.

1. INTRODUCTION

Matched-field processing (MFP) has been shown to be an effective technique for source localization in shallow water, but it can be extremely sensitive to errors in the assumed values of the environmental parameters [1]. This sensitivity to environmental mismatch is proportional to frequency. Thus, MFP is typically applied to low frequency signals, e.g., < 300 Hz, where sensitivity is smallest. Environmentally robust MFP algorithms have been developed which are insensitive to certain levels of environmental uncertainty [2]. However, these algorithms were also applied to signals in the low-frequency range. Thus development of robust MFP algorithms for mid-frequency signals, e.g., $800 - 3000$ Hz, is a largely unexplored topic.

Another issue in the application of MFP is array length and density of elements. The perfect array for MFP is one that spans the water column and is densely populated with elements. This provides a complete sampling of the mode-functions which results in low sidelobe levels on the range-depth ambiguity surface. However, in many applications the use of a long array is impractical and short arrays must be considered. Because short arrays only span a small segment of the water column, they generally undersample the mode-functions. This can result in large sidelobes on the range-depth ambiguity surface computed at a single frequency. Sidelobe height is inversely proportional to array length. Incoherently averaging ambiguity surfaces computed at multiple frequencies across the signal band can help alleviate this problem to some degree. Again, most of the robust MFP algorithms described in the literature are demonstrated using long arrays with many sensors. The application of robust MFP algorithms using a 23 meter, 5-element vertical array at frequencies of $100 - 600$ Hz in simulated environments with relatively small levels of uncertainty is given in [3] and [4].

In this paper, we present an MFP algorithm that is robust to moderate amounts of environmental uncertainty for the challenging problem of localization using mid-frequency signals received on extremely short vertical-arrays. Previously we derived the L_∞-norm estimator from the interpretation of the maximum *a posteriori* (MAP) estimator as an exponentially-weighted averaging processor [5], [6]. The MAP estimator is a statistically optimal approach to robust source localization in the limit of infinite averaging. With MAP, the uncertain environmental parameters are treated as nuisance parameters and are averaged over in the process of estimating source location. Simulated and experimental data results were presented in [6] using long vertical arrays and narrowband signals which demonstrated for finite averaging that the L_∞-norm estimator provided superior localization performance over that of MAP. We now apply a broadband L_∞-norm estimator to this new paradigm and illustrate why it is even better suited to the solution of this problem than MAP. In support of these assertions, we present realistic simulation results using signals in the band of $1000 - 3000$ Hz received on a 3-meter vertical array which demonstrate the significant performance gains in using the L_∞-norm estimator over MAP and the conventional Bartlett processor.

2. ALGORITHM DEVELOPMENT

2.1. Signal model

The signals from a point source received on a vertical array of N sensors can be expressed in vector form as

$$\mathbf{y}(\omega) = s(\omega)\mathbf{a}(\omega, \Theta, \Psi) + \mathbf{n}(\omega) \quad (1)$$

where the elements of the received data vector $\mathbf{y}(\omega)$ are the components of the signal wavefront observed on the sensors located at depths $\mathbf{z} = [z_1^T, \ldots, z_N^T]^T$ at radian frequency ω. The scalar $s(\omega)$ is the complex signal amplitude at ω. The signal *replica vector* $\mathbf{a}(\omega, \Theta, \Psi)$ is the acoustic transfer function between a source at location $\Theta = [r, z]$ and the array, while the vector Ψ contains the values of the environmental parameters, i.e., sound-velocity profile and bottom characteristics. The vector $\mathbf{n}(\omega)$ contains samples of complex, Gaussian noise.

This work was supported by the Office of Naval Research, ONR321US.

2.2. Broadband L_∞-norm estimator

A wideband MAP estimator was derived in [7]. If we assume that the replica vectors are normalized to unit norm and that the noise is white, we can express this MAP estimator as

$$\widehat{\Theta} = \arg\max_{\Theta} \int_{\Psi} \exp\left\{ \sum_{l=1}^{L} \frac{\sigma_a^2 \left| \mathbf{a}^H(\omega_l, \Theta, \Psi)\mathbf{y}(\omega_l) \right|^2}{2(\sigma_a^2 + 1)} \right\} p(\Psi)\, d\Psi, \tag{2}$$

where σ_a^2 is the signal amplitude variance at the source, and $p(\Psi)$ is the prior probability density function of the uncertain environmental parameters which is assumed to be uniformly distributed. The uncertainty bounds of the environmental parameters are determined from *in situ* measurements and historical data. Practical application of (2) requires the integral to be approximated numerically which results in

$$\widehat{\Theta} = \arg\max_{\Theta} \sum_{i=1}^{M} \exp\left\{ \sum_{l=1}^{L} \frac{\sigma_a^2 \left| \mathbf{a}^H(\omega_l, \Theta, \Psi_i)\mathbf{y}(\omega_l) \right|^2}{2(\sigma_a^2 + 1)} \right\}. \tag{3}$$

The integration is approximated by a summation over M realizations of the environmental parameters. Observe that the argument of the exponential in (3) is the multi-frequency Bartlett processor scaled by $\frac{\sigma_a^2}{2(\sigma_a^2+1)}$. Thus (3) is simply an exponentially-weighted average, over M realizations of the environment, of multi-frequency Bartlett surfaces. If we assume $\mathbf{y}(\omega_l)$ is also normalized to unit norm, and Θ and Ψ_i are perfectly matched to the data, then $\left| \mathbf{a}^H(\omega_l, \Theta, \Psi_i)\mathbf{y}(\omega_l) \right|^2$ would equal one. Any other values of Θ and Ψ_i would result in a value between zero and one. Since a perfect match would be consistent over frequency, this would result in the argument of the exponential equaling $\frac{L\sigma_a^2}{2(\sigma_a^2+1)} \approx \frac{L}{2}$. Thus the range of values for the argument of the exponential would be zero to $\frac{L}{2}$. Values of $\left| \mathbf{a}^H(\omega_l, \Theta, \Psi_i)\mathbf{y}(\omega_l) \right|^2$ nearer to one, which correspond to *better* replica-data matches, result in values of the exponential argument closer to $\frac{L}{2}$. Therefore with the non-linear exponential weighting, multi-frequency Bartlett surfaces from environmental realizations Ψ_i which are better matches to the data receive more relative weight in the averaging process.

The exact implementation of the MAP estimator in (2) *integrates* over environmental realizations, which is equivalent to computing (3) with infinitesimally-spaced samples of the environmental parameters, i.e., $M \to \infty$. Thus, the true environment and realizations close to the true are all included in the averaging process, which results in a clustering of reinforcing peaks in the vicinity of the true value of Θ. However, due to processing time and computational constraints only a finite number of environmental realizations can be used in practice. A reasonable number of environmental realizations for practical application would be on the order of $100 - 200$. Therefore, the practical implementation of MAP in (3) can be suboptimal.

Finite sampling of the environmental parameter space results in a smaller number of better replica-data matches. Therefore, there is a reduced occurrence of the clustering of peaks in the vicinity of the true source location Θ using the MAP estimator. This increases the possibility of the true peak being averaged out and obscured by sidelobes reinforced over the averaging process. As we shall see, this is especially true for short arrays and mid-frequency signals. As developed in [5] and [6] using narrowband signals, we can compensate for this by giving better replica-data matches more relative weight in the averaging process. This can be accomplished by replacing the exponential weighting in (3) with a p-power weighting, i.e., replacing $\exp\{x\}$ by $\{x\}^p$, which results in essentially an L_p norm over environment. In the limit as $p \to \infty$, the broadband L_∞-norm estimator, given by

$$\widehat{\Theta} = \arg\max_{\Theta, \Psi_i} \sum_{l=1}^{L} \left| \mathbf{a}^H(\omega_l, \Theta, \Psi_i)\mathbf{y}(\omega_l) \right|^2 \quad i = 1, 2, \ldots, M, \tag{4}$$

simply finds the best match over source location Θ using the M realizations of the environmental parameters. Since it is extremely unlikely that the true values of the environmental parameters are included in the M realizations, the L_∞-norm estimator of (4) inherently assumes that other combinations of the environmental parameters can produce accurate localization estimates.

In our previous work [5], [6], we showed that this assumption is valid. It was observed that localization processing is most sensitive to mismatch in the assumed values of the horizontal wavenumbers. The horizontal wavenumbers are a function of environment and frequency, and comprise the phase of the replica vectors. Using a modal decomposition of the replica vectors, we showed that the localization process is only dependent on the set of relative differences between the wavenumbers for a given environment and not their precise values. Thus, a combination of the environmental parameters generating a wavenumber set which produces a set of wavenumber differences that is nearly identical to those for the true environment will result in a nearly identical localization estimate. We also introduced the concept of a wavenumber gradient (WG) as a metric for quantifying the similarity of environmental realizations. The WG is simply the gradient of the curve obtained by connecting the wavenumbers for a particular environmental realization by line segments. Curves with nearly identical gradients will have nearly identical relative wavenumber differences. In simulation studies, we demonstrated that environmental realizations having nearly identical WG's produced nearly identical localization results. Recently we have observed that the WG is consistent over frequency. That is, the error between the WG's for two given environmental realizations is relatively constant over frequency. Thus, an environmental realization producing a nearly correct localization estimate does so across all frequencies and is positively reinforced by the frequency averaging of the broadband L_∞-norm estimator. This is a topic of current investigation.

3. ISSUES RELATED TO SHORT ARRAYS AND MID-FREQUENCY SIGNALS

In this section we will describe and demonstrate the effects of short arrays and mid-frequency signals on MFP. The sensitivity of MFP to environmental mismatch is greater using mid-frequency signals. This is due to the fact that the main-lobe width of the peak of the range-depth ambiguity surface is inversely proportional to frequency. When mismatch is introduced, the peak of this surface moves along the main lobe away from its apex when no mismatch was present. Thus, good localization results are obtained provided the peak shifts to a point on the main lobe which is greater than any of the sidelobes. Large localization errors occur once the mismatch is large enough such that the peak shifts to a point away from the main lobe. Because low frequency signals produce wider main-lobe widths, the application of MFP using these signals can tolerate larger amounts of environmental uncertainty.

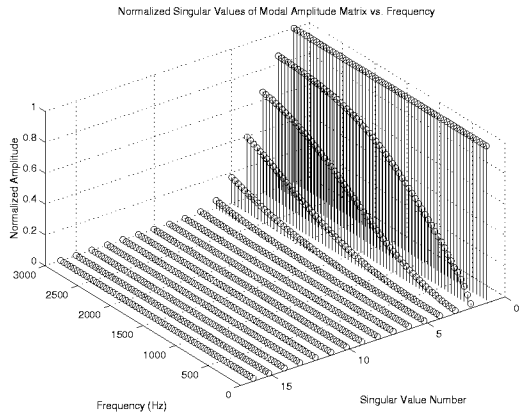

Figure 1: Singular values of modal amplitude matrix vs. frequency.

However, we can show that MFP using short arrays is better suited to mid-frequency signals. Using a modal representation, the signal replica vector can be decomposed as the matrix-vector product

$$\mathbf{a}(\omega, \Theta, \Psi) = \Omega(\omega, \mathbf{z}, \Psi)\alpha(\omega, \Theta, \Psi), \tag{5}$$

where the columns of the $N \times Q$ modal amplitude matrix $\Omega(\omega, \mathbf{z}, \Psi)$ are the Q mode-functions sampled at the receiver depths and $\alpha(\omega, \Theta, \Psi)$ is a vector of complex weights. All of the replica vectors lie in the subspace generated by the columns of $\Omega(\omega, \mathbf{z}, \Psi)$. When a very short array is used for MFP the modefunctions are undersampled and $\Omega(\omega, \mathbf{z}, \Psi)$ can become rank deficient. This reduction in the dimensionality of the subspace results in increased sidelobes on the range-depth ambiguity surface. In the limit as the rank approaches one, all of the replica vectors become co-linear. Thus, all of the hypothesized source locations Θ produce the same estimator output resulting in a flat range-depth ambiguity surface.

To illustrate this point, we will demonstrate how the rank of $\Omega(\omega, \mathbf{z}, \Psi)$ changes with frequency using a small aperture vertical array. In Figure 1, a plot of the singular values of $\Omega(\omega, \mathbf{z}, \Psi)$ versus frequency for the shallow-water environment described in Section 4 using a 3-meter vertical array with 16 equally spaced elements is presented. The number of significant singular values is equivalent to the rank of a matrix. Notice that at frequencies below 500 Hz, the rank is nearly one. The rank increases beyond one as the frequency increases above 500 Hz. The reason for this is that as frequency is increased, more higher-order modes begin to propagate. With such a short vertical aperture, the lower-order modes appear as a constant amplitude across the array. These higher-order modes, which produce increasingly greater numbers of amplitude oscillations across the array, are responsible for increasing the dimension of the subspace. When using a short array for MFP, higher frequencies can provide better localization performance provided a robust estimator is utilized.

We can demonstrate the combined effects of using a short array with mid-frequency signals for MFP, again using the environment described in Section 4. We will do this using the conventional Bartlett processor in the presence of environmental mismatch with a 95 meter and a 3-meter array. Each array contained 16 equally spaced elements. A noise-free data vector was generated for a fixed source location of 3000 m in range and 50 m in depth using the nominal values of the environmental parameters

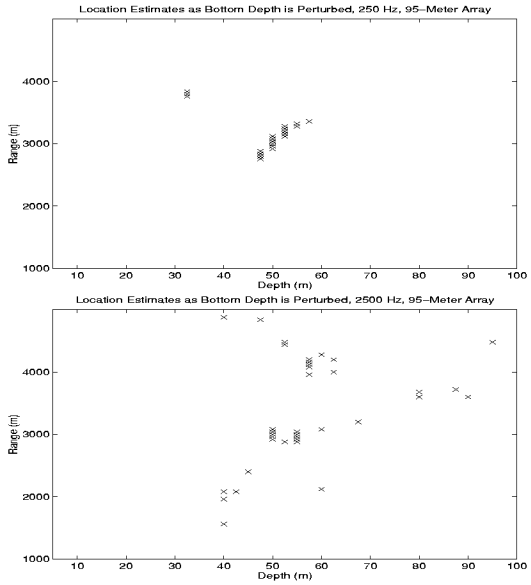

Figure 2: Scatter plots of Bartlett peaks using a 95-meter array at 250 Hz (top) and 2500 Hz (bottom).

given in Table 1 at frequencies of 250 Hz and 2500 Hz. Water depth was assumed to be the only uncertain environmental parameter. A set of 100 localization estimates were computed for the arrays at both frequencies. In computing the 100 estimates for each of the four configurations, the Bartlett processor assumed 100 unique, randomly selected water depths from the interval of 114 ± 5 meters. In Figures 2 and 3, scatter plots of the peak outputs of the Bartlett processor for the 100 trials in each of the configurations are shown. Figure 2 shows the results for the 95-meter array. At 250 Hz, most of the points are clustered about the true source location, while at 2500 Hz there is a small amount of clustering around the true source location. In contrast, Figure 3 shows the results for the 3-meter array. We see that at 250 Hz there is very little clustering and at 2500 Hz the points are distributed throughout the search region. Therefore, the MAP estimator, which relies on clustering for good performance, would have very little success operating with a small aperture array in this scenario. Since the L_∞-norm estimator simply finds the best overall match and is not dependent on clustering, it is better suited to this problem.

4. SIMULATION RESULTS

The performance of the broadband L_∞-norm estimator was compared to that of the wideband MAP and Bartlett processors using a realistic simulated environment modeled after a region in the Gulf of Mexico [8]. This is a 3-layer shallow-water environment comprised of water over sediment over rock. An actual measured sound-velocity profile (SVP) from the Gulf of Mexico was used in the simulations. SVP uncertainty for the simulations was created by modeling the SVP as $c(z) = g\varphi(z) + c_o(z)$, where $c_o(z)$ was the actual measured SVP, $\varphi(z)$ was a perturbation vector, and g, the uncertain component of the SVP, was a random variable uniformly distributed between 0 and 0.35. The six other environmental parameters assumed for this environment and their uncertainty intervals are shown in Table 1. The receiving array consisted of

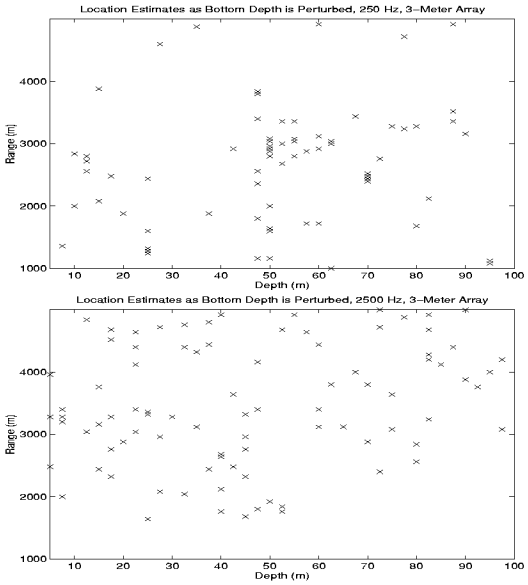

Figure 3: Scatter plots of Bartlett peaks using a 3-meter array at 250 Hz (top) and 2500 Hz (bottom).

Parameter	Uncertainty Interval
water depth	114 ± 5 m
sediment sound speed	1600 ± 37.5 m/s
rock sound speed	1625 ± 37.5 m/s
sediment attenuation	0.5 ± 0.25 dB/λ
sediment density	1.85 ± 0.25
rock density	2.2 ± 0.25

Table 1: Ranges of environmental uncertainty for Gulf of Mexico environment.

16 equally-spaced elements with a total aperture of 3 meters. The top element of the array was located at a depth of 40 meters. The estimators used 17 frequency components equally spaced across the band of $1000 - 3000$ Hz in processing.

Localization performance was tested using 100 Monte Carlo trials for signal-to-noise ratios (SNR) of -5 dB to 40 dB. The range-depth search region was $1000 - 6000$ m in range and $10 - 100$ m in depth. The trials consisted of 100 synthesized data observations, each generated using a unique randomly selected source location and environmental realization sampled from the uncertainty intervals of the environmental parameters. The appropriate level of zero-mean, Gaussian noise was then added to the data for each SNR. The L_∞ norm and MAP estimators processed the data using an independent set of $M = 200$ randomly selected environmental realizations, while the Bartlett processor assumed the nominal values of the environmental parameters. A correct localization was defined as an estimate within a region of ± 300 m in range and ± 4 m in depth of the true source location. Figure 4 presents the simulation results which show that the L_∞-norm estimator provides a significant performance improvement over that of MAP and Bartlett. As discussed previously, the performance of MAP suffers from the lack of clustering at these frequencies with finite environment sampling. The dismal performance of Bartlett stems from the narrow main-lobe widths produced at these

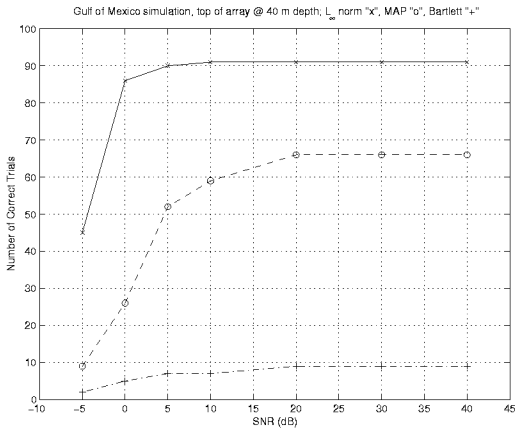

Figure 4: Simulation results; L_∞ norm - x, MAP - o, Bartlett - +.

frequencies which provide little tolerence for mismatch combined with the poor peak-to-sidelobe ratio for a 3-meter array.

5. CONCLUSION

This paper demonstrated that MFP with a very short array using mid-frequency signals is feasible provided a robust estimator is used. The broadband L_∞-norm estimator was shown to be the most effective processor for the solution to this problem as compared to the MAP and Bartlett processors.

6. REFERENCES

[1] A.B. Baggeroer, W.A. Kuperman, and P.N. Mikhalevsky, "An overview of matched field methods in ocean acoustics," *IEEE J. of Oceanic Eng.*, vol. 18, pp. 401-424, 1993.

[2] J.P. Ianniello, "Recent developments in sonar signal processing," *IEEE Signal Proc. Mag.*, vol. 15, no. 4, pp. 27-40, 1998.

[3] B.F. Harrison, R.J. Vaccaro, and D.W. Tufts, "Robust broadband matched-field localization: Results for a short, sparse vertical array," submitted to *J. Acoust. Soc. Am.*, 1998.

[4] S.P. Czenszak and J.K. Krolik, "Robust wideband matched-field processing with a short vertical array," *J. Acoust. Soc. Am.*, vol. 101, pp. 749-759, 1997.

[5] B.F. Harrison and J.L. Harrison, "Robust matched-field processing in uncertain shallow-water environments using an L_p-norm estimator," in *Proc. ICASSP 1998*, vol. 4, pp. 2441-2444, 1998.

[6] B.F. Harrison, "An L_∞-norm estimator for environmentally robust, shallow-water source localization," to appear *J. Acoust. Soc. Am.*, January 1999.

[7] J.A. Shorey and L.W. Nolte, "Wideband optimal *a posteriori* probability source localization in an uncertain shallow ocean environment," *J. Acoust. Soc. Am.*, vol. 103, pp. 355-361, 1998.

[8] J. Ianniello, "A MATLAB version of the KRAKEN normal mode code," technical report TM 94-1096, Naval Undersea Warfare Center, October 1994.